

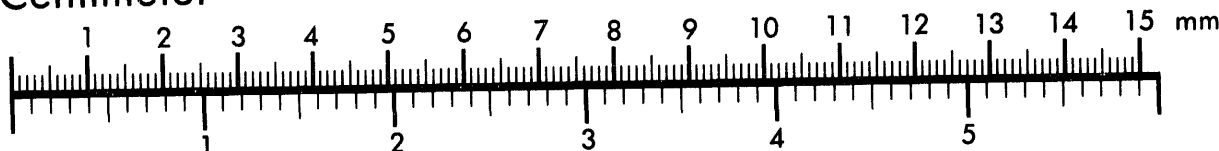


**AIIM**

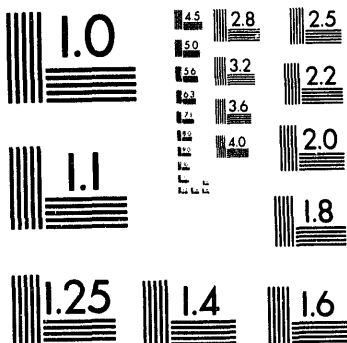
**Association for Information and Image Management**

1100 Wayne Avenue, Suite 1100  
Silver Spring, Maryland 20910  
301/587-8202

**Centimeter**



**Inches**



MANUFACTURED TO AIIM STANDARDS  
BY APPLIED IMAGE, INC.

1 of 1

Conf-940507--6  
ANL/TP/CP--81180

The submitted manuscript has been authored by a contractor of the U.S. Government under contract No. W-31-109-ENG-38. Accordingly, the U.S. Government retains a nonexclusive, royalty-free license to publish or reproduce the published form of this contribution, or allow others to do so, for U.S. Government purposes.

## Nuclear Data Needs and Sensitivities for Illicit Substance Detection Using Fast-Neutron Transmission Spectroscopy

B. J. Micklich, M. K. Harper, L. Sagalovsky, and D. L. Smith  
Technology Development Division  
Argonne National Laboratory  
Argonne, Illinois USA 60439  
708/252-4849

### ABSTRACT

Results from analysis of fast-neutron transmission spectra in the interrogation of luggage for illicit substances are quite sensitive to the neutron total cross section data employed. Monte Carlo and analytical techniques are used to explore the uses for such data and to demonstrate the sensitivity of these results to various total cross sections employed in the analysis. The status of total cross section information required for materials commonly found in containers having both illicit and benign substances, with particular attention to the matter of data uncertainties, is considered in the context of the available nuclear data. Deficiencies in the contemporary nuclear data base for this application are indicated and suggestions are offered for new measurements or evaluations.

### I. INTRODUCTION

Fast-neutron interrogation techniques are of interest in the detection of illicit substances such as explosives because of their ability to identify light elements such as carbon, nitrogen, and oxygen, which are the primary constituents of these materials, based on unique features of their nuclear signatures. Fast-neutron transmission spectroscopy (FNTS) uses standard time-of-flight (TOF) techniques to measure the energy spectrum of neutrons emitted from a collimated continuum source before and after transmission through an object being interrogated. An unfolding algorithm is then used to determine the areal densities (number density per  $\text{cm}^2$ ), and the uncertainties, of various elements present in the sample. The areal densities are then processed into normalized areal densities (relative to the number density for all elements considered) of hydrogen, carbon, nitrogen, and oxygen, which are used to determine the presence of an explosive.

### II. UNFOLDING ALGORITHM

The Monte Carlo transport code MCNP<sup>1</sup> was used to simulate transmission of fast neutrons from a  $^9\text{Be}(\text{d},\text{n})$  source<sup>2</sup> [ $E_d = 5 \text{ MeV}$ ] through a variety of benign and explosive materials. The resulting TOF spectra were analyzed to extract the elemental areal densities from the transmission spectra based on the neutron total cross sections and their covariances. The algorithm is similar to the method of effective variance<sup>3</sup> and is written as<sup>4</sup>

$$\begin{aligned} \mathbf{V}_p &= (\mathbf{A}^T \mathbf{V}_y^{-1} \mathbf{A})^{-1} \\ \mathbf{p} &= \mathbf{V}_p \mathbf{A}^T \mathbf{V}_y^{-1} \mathbf{y} \\ \chi^2 &= (\mathbf{y} - \mathbf{Ap})^T \mathbf{V}_y^{-1} (\mathbf{y} - \mathbf{Ap}) \end{aligned} \quad (1)$$

Here  $\mathbf{y}$  = vector of transmission ratios [ $y_i = \ln(N_{0i}/N_i)$ ]  
 $\mathbf{V}_y$  = covariance matrix for  $\mathbf{y}$   
 $\mathbf{A}$  = total cross section matrix [ $A_{ik} = \sigma_k(E_i)$ ]  
 $\mathbf{p}$  = solution vector  
 $\mathbf{V}_p$  = covariance matrix for  $\mathbf{p}$

The covariance matrix  $\mathbf{V}_y$  is calculated by

$$\begin{aligned} (\mathbf{V}_y)_{ij} &= \delta_{ij} [(1/N_{0i}) + (1/N_i)] \\ &+ \sum_{k=1}^m p_k^2 (C_k)_{ij} v_{ki} \sigma_{ki} v_{kj} \sigma_{kj} \end{aligned} \quad (2)$$

where  $\sigma_{ki}$  are the total cross sections  
 $v_{ki}$  are the fractional errors in the  $\sigma_{ki}$   
 $C_k$  is the correlation matrix for the set  $\sigma_{ki}$

The method evaluates the equations (1) in an iterative fashion, with  $\mathbf{V}_y$  in the initial pass being calculated using only the errors in the counting statistics (i.e., for  $\mathbf{p} = 0$ ).

MASTER  
DISTRIBUTION OF THIS DOCUMENT IS UNLIMITED

## **DISCLAIMER**

This report was prepared as an account of work sponsored by an agency of the United States Government. Neither the United States Government nor any agency thereof, nor any of their employees, makes any warranty, express or implied, or assumes any legal liability or responsibility for the accuracy, completeness, or usefulness of any information, apparatus, product, or process disclosed, or represents that its use would not infringe privately owned rights. Reference herein to any specific commercial product, process, or service by trade name, trademark, manufacturer, or otherwise does not necessarily constitute or imply its endorsement, recommendation, or favoring by the United States Government or any agency thereof. The views and opinions of authors expressed herein do not necessarily state or reflect those of the United States Government or any agency thereof.

Calculating the normalized areal densities and their errors yields a solution like that shown in Figure 1 for a 3-cm thick sample of the explosive RDX under representative exposure conditions.<sup>5</sup> The solution is characterized by a point giving the normalized areal densities (here shown in two dimensions) and an ellipse giving the location of points which lie one standard deviation away (called the 1- $\sigma$  ellipse). The second pass through the algorithm adjusts the areal densities slightly, but its main effect is to increase the standard deviations since the cross-section errors are now taken into account. The accuracy of the unfolding is indicated in Figure 3, which shows that the differences between the data points and the fit to the data are consistent with the standard deviations in the data due to counting statistics (about two percent in the range 1-5 MeV and somewhat larger outside this range). The figure also shows that the transmission based on the calculated areal densities compares favorably with the transmission based on the actual areal densities. Covariance data are not present in the evaluations for several elements (H, N, O, Cl, and Na) and were approximated using data from Ref. 6. Good covariance data are necessary to correctly calculate the uncertainties in areal densities, which are used in subsequent probabilistic interpretation of the results.<sup>7</sup>

### III. TRANSMISSION-DERIVED CROSS SECTIONS

The quality of the results from unfolding depends on using the correct set of cross sections in the  $\mathbf{A}$  matrix. In particular, it is necessary to use cross sections obtained from simulated transmission experiments (transmission-derived cross sections) rather than energy-averaged cross sections. Energy-averaged cross sections are calculated by averaging the total cross sections over the TOF energy bins using a flat weighting function. Transmission-derived cross sections are obtained by calculating the transmission for single-material samples and inverting the TOF spectra. In such a transmission simulation, the errors in the resulting cross sections depends on the transmission.<sup>8</sup> Assuming  $T = \exp[-x]$ , we find that

$$\begin{aligned}\Delta x / x &= (\Delta T / T) \cdot (1/x) \\ &= \exp[-x/2] / x\end{aligned}\quad (3)$$

which is minimum when  $x=2$ , or  $T=0.135$ . Figure 2 shows the dependence of relative error in the total cross section on transmission.

Since the relative error has a broad minimum for transmissions in the range 0.1-0.4, the samples were chosen so that the average transmission would be approximately 0.3, for which the relative error is 1.12

times the minimum. At cross section resonances, where the transmission would be lower, the transmission stays in a range where the resulting cross section error will be relatively small. For example, if the cross section is such that  $T = 0.3^2 = 0.09$ , the relative cross section error would be 1.02 times the minimum. At a resonant window where the transmission might be, for example,  $0.55 = \sqrt{0.3}$ , the relative error would be 1.65 times the minimum. By using the appropriate sample thickness and running enough histories, the statistical error in the simulation is made small compared to the errors in the cross sections themselves.

Figure 4 shows a comparison between the energy-averaged and transmission-derived total cross sections for carbon. The energy-averaged cross section is higher than that obtained by transmission at the peaks of several resonances, leading to a value of areal density which is too low. Lowering the total cross section at these resonance peaks by 20% increases the calculated carbon areal density by 20%. This indicates that the unfolding algorithm is extremely sensitive to the cross section resonances (i.e., the unique features for each element). These observations for carbon hold equally well for other elements of interest (e.g., oxygen and nitrogen). In particular, the fits for oxygen are better than those for other elements (in terms of both accuracy and lower standard deviation) because of the broad, deep resonance window at 2.35 MeV.

### IV. TOTAL CROSS-SECTION COMPARISON

The total cross sections for the elements carbon, nitrogen, and oxygen are shown in Figures 5-7 in the form of plots which give the differences between ENDF/B-5<sup>9</sup> and either ENDF/B-6<sup>10</sup> or ENDL-90.<sup>11</sup> ENDF/B-5 is used as the standard because that evaluation constitutes the bulk of the currently recommended cross sections for MCNP. ENDF/B-5 and ENDF/B-6 are generally within a few percent of each other, except for oxygen in which there are a number of larger differences, sometimes as much as 40-60%, at some of the sharp resonances. The differences between ENDL-90 and ENDF-5 are larger, due to the fact that for these elements ENDL-90 uses many fewer data points over the energy range 0.5-10 MeV, and does not represent a number of the very narrow resonances.

When transmission-derived cross sections are generated for use in the unfolding algorithm, the differences between data libraries are much smaller. These differences are shown for carbon cross sections calculated from ENDF-5 and ENDL-90 in Figure 8. The narrow resonances which are missing from ENDL-90 are

washed out in the transmission-derived cross sections because of the energy-averaging inherent in the TOF bin structure. We expect that differences in transmission-derived cross sections between ENDF-5 and ENDF-6 would be smaller.

To test the sensitivity of calculated areal densities to the use of different data libraries, the neutron transmission through 3-cm thick RDX was simulated using cross sections from ENDL-90 and analyzed using transmission-derived cross sections based on ENDL-90. Figure 9 compares the transmission spectrum to that obtained using ENDF-5. The differences between the spectra are much smaller than one would expect based only on examining the pointwise cross sections, and are consistent with counting statistics. There is a slightly lower transmission for ENDL-90 at energies beneath 1 MeV, probably due to higher cross sections for carbon and oxygen in this range. The areal densities for all elements included in the A matrix are virtually identical and agree within the calculated uncertainties. Small differences are expected between results using ENDF-5 and ENDF-6.

## V. CONCLUSIONS AND RECOMMENDATIONS

The use of transmission-derived rather than energy-averaged cross sections is essential to correct unfolding of elemental densities from transmission data. The areal densities calculated using ENDF and ENDL data agree within statistics when the same data library is used in both the transmission simulations and analysis.

Although much effort has been put into cross section evaluation, the accumulated data base still requires improvement for this particular application. Evaluations for several elements important for illicit substance detection (e.g., Na, Al, Si, Cl, K) have not been updated in quite some time (see Table 1). The overall quality of neutron transmission simulations would be improved most by making new measurements and evaluations for these elements, including resolved resonances in the MeV region. Covariance data need to be provided for those elements for which they are lacking, especially hydrogen, nitrogen, and oxygen. The quality of the existing covariance data is questionable in several other cases (Na, Al, Si).

## ACKNOWLEDGMENTS

This work was supported by the Federal Aviation Administration Technical Center under contract DTFA03-03-X-00021. M. K. Harper was supported by the Student Research Participation Program administered by Argonne's Division of Educational Programs.

## REFERENCES

1. J. W. Meadows, "The Thick-Target  $^9\text{Be}(\text{d},\text{n})$  Neutron Spectra for Deuteron Energies Between 2.6 and 7.0 MeV," ANL/NDM-124 (Nov. 1991).
2. 'MCNP - A Generalized Monte Carlo Code for Neutron and Photon Transport, Version 3A,' LA-7396-M, Rev. 2, Los Alamos National Laboratory (Sept. 1986).
3. J. Orear, *Amer. J. Phys.* **50**, pp. 912-916 (1982).
4. D. L. Smith, ANL/NDM-62 (Nov. 1982).
5. B. J. Micklich, M. K. Harper, A. H. Novick, and D. L. Smith, 8th Symposium on Radiation Measurements and Applications, Ann Arbor, MI (May 1994).
6. V. McLane, C. L. Dunford, and P. Rose, 'Nuclear Cross Sections, Vol. 2: Neutron Cross Section Curves,' Academic Press, San Diego, CA (1988).
7. D. L. Smith, L. Sagalovsky, B. J. Micklich, M. K. Harper, and A. H. Novick, 4th Int'l Conference on Applications of Nuclear Techniques, Crete, Greece (June 1994).
8. E. J. Burge, *Nucl. Instr. Meth.* **144**, pp. 547-555 (1977).
9. R. Kinsey, 'ENDF/B-5 Summary Documentation,' BNL-NCS-17541, (ENDF-201, 3rd Ed.) (Jul. 1979).
10. P. F. Rose, 'ENDF/B-6 Summary Documentation,' BNL-NCS-17541, (ENDF-201, 4th Ed.) (Oct. 1991).
11. LLNL Nuclear Data Section, 'ENDL-90, Evaluated Nuclear Data Library'.

Table 1. Characteristics of ENDF/B-6.

element	latest revision date	total xsec covariance?	element/isotope?
H	10/89	N	I
C	8/89	Y	E, I <sup>a</sup>
N	9/92	N	I
O	1/90	N	I
F	6/90	Y	I <sup>b</sup>
Na	12/77	Y	I <sup>b</sup>
Al	12/73	Y	I <sup>b</sup>
Si	2/74	Y	E
Cl	2/67	N	E
K	2/67	N	E
Fe	11/89	Y	I
Cu	11/89	Y	I

<sup>a</sup>Cross sections available both by element and isotope

<sup>b</sup>Element has only one naturally occurring isotope

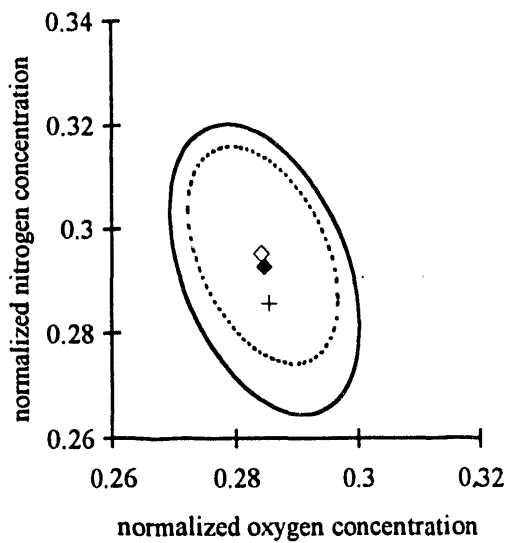


Figure 1. Results from the element unfolding algorithm for 3 cm RDX explosive and 1.4 million source neutrons. The plus sign represents the true solution, the open diamond and dashed line represent the first-pass solution, and the filled diamond and solid line represent the second pass solution. The curves give the points which are  $1-\sigma$  away from the solution point.

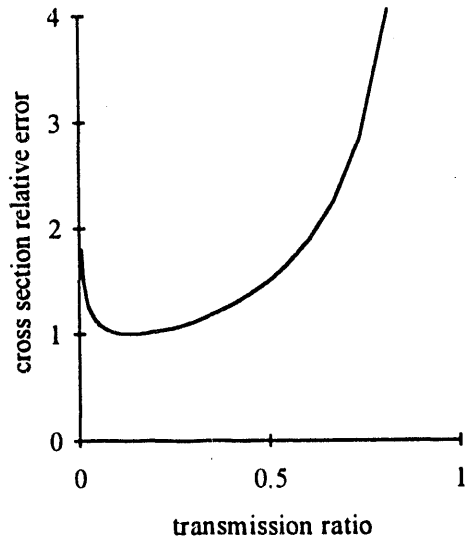


Figure 2. Cross section error relative to the minimum error vs. transmission ratio for cross section measured with transmission measurement (simulation). The optimum transmission ratio is  $\exp[-2] = 0.135$ .

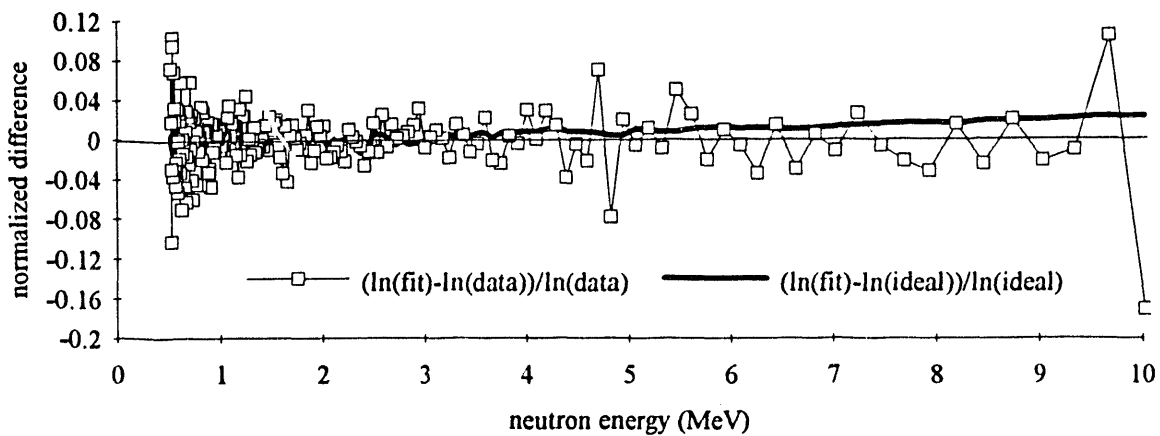


Figure 3. Difference plots showing transmission data points, the transmission based on the fit to the data, and the transmission based on the actual elemental areal densities.

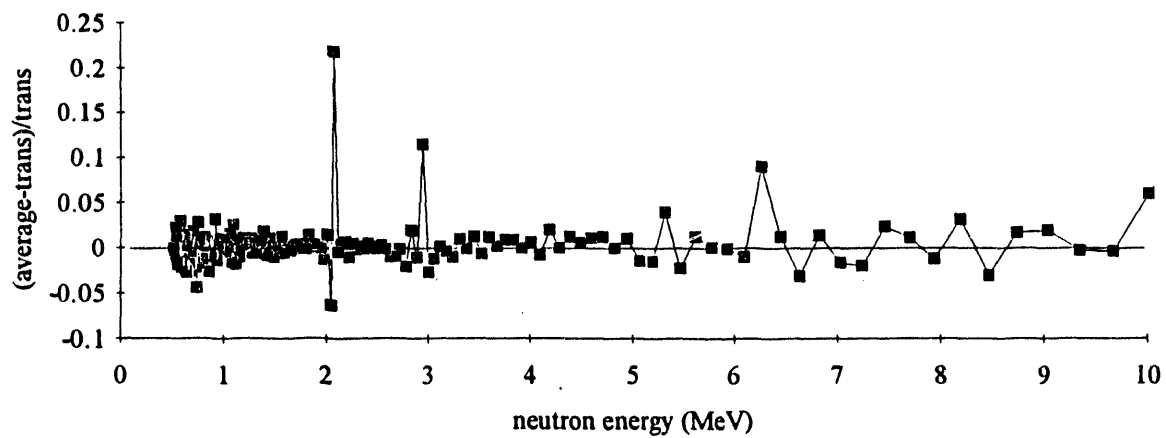


Figure 4. Difference plot for energy-averaged and transmission-derived total carbon cross sections from ENDF/B-5 evaluation.

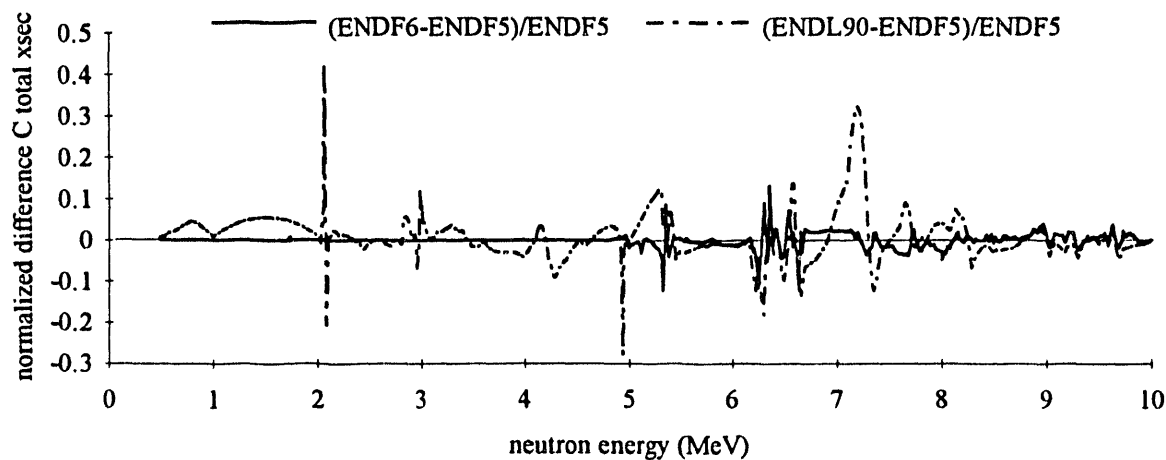


Figure 5. Difference plot of carbon total cross section from ENDF/B-6 and ENDL-90 relative to ENDF/B-5.

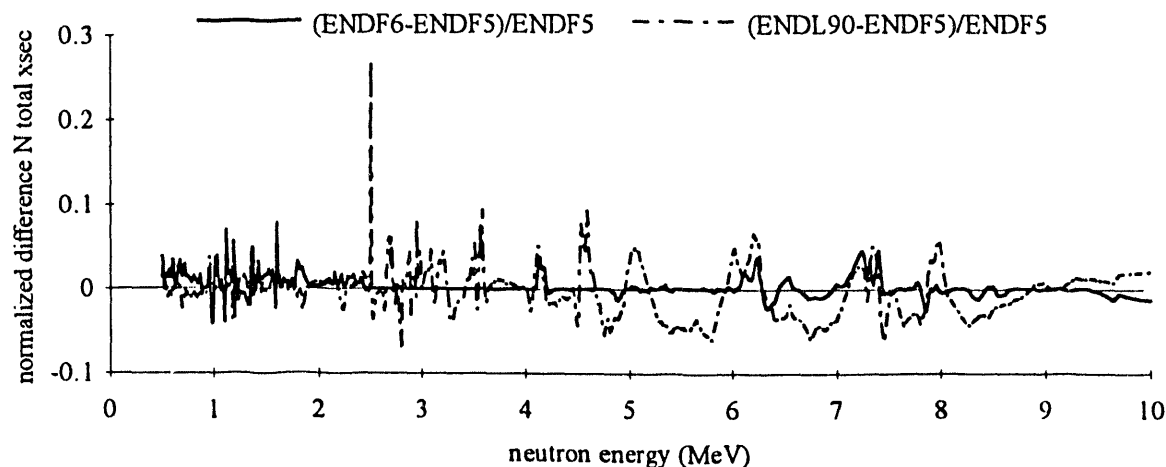


Figure 6. Difference plot of nitrogen total cross section from ENDF/B-6 and ENDL-90 relative to ENDF/B-5.

1995/11/26

DATE  
MEDLINE

